JACS
JOURNAL OF THE AMERICAN CHEMICAL SOCIETY

Article

pubs.acs.org/JACS

Cell-Selective Biological Activity of Rhodium Metalloinsertors Correlates with Subcellular Localization

Alexis C. Komor, Curtis J. Schneider, Alyson G. Weidmann, and Jacqueline K. Barton*

Division of Chemistry and Chemical Engineering, California Institute of Technology, Pasadena, California 91125, United States

Supporting Information

ABSTRACT: Deficiencies in the mismatch repair (MMR) pathway are associated with several types of cancers, as well as resistance to commonly used chemotherapeutics. Rhodium metalloinsertors have been found to bind DNA mismatches with high affinity and specificity *in vitro*, and also exhibit cell-selective cytotoxicity, targeting MMR-deficient cells over MMR-proficient cells. Ten distinct metalloinsertors with varying lipophilicities have been synthesized and their mismatch binding affinities and biological activities determined. Although DNA photocleavage experiments demonstrate that their binding affinities are quite similar, their cell-selective antiproliferative and cytotoxic activities vary significantly. Inductively coupled plasma mass spectrometry (ICP-MS) experiments have uncovered a relationship between the subcellular distribution of these metalloinsertors and their biological activities. Specifically, we find that all of our metalloinsertors localize in the nucleus at sufficient concentrations for binding to DNA mismatches. However, the metalloinsertors with high rhodium localization in the mitochondria show toxicity that is not selective for MMR-deficient cells, whereas metalloinsertors with less mitochondrial rhodium show activity that is highly selective for MMR-deficient versus proficient cells. This work supports the notion that specific targeting of the metalloinsertors to nuclear DNA gives rise to their cell-selective cytotoxic and antiproliferative activities. The selectivity in cellular targeting depends upon binding to mismatches in genomic DNA.

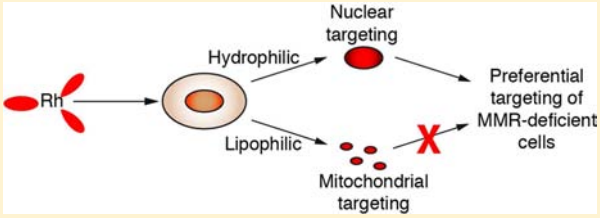

INTRODUCTION

The cell has evolved a complex replication mechanism containing multiple checkpoints in order to minimize the incorporation of errors during replication and correct errors that result from chemical damage to DNA after replication.[1] Left uncorrected, these DNA defects will lead to mutations in subsequent rounds of replication.[2,3] The mismatch repair (MMR) pathway provides one such checkpoint and increases the fidelity of DNA replication ~1000-fold.[4] Not surprisingly, defects in this pathway have been associated with several types of cancer. For example, about 18% of solid tumors and 15% of sporadic colorectal cancer cases have been found to exhibit MMR deficiencies.[5,6] Furthermore, many commonly used chemotherapeutics, such as cisplatin, DNA alkylating agents, and antimetabolites, have decreased effectiveness against MMR-deficient cancer cells.[7] In fact, repeated chemotherapeutic treatments with these agents enrich tumors with MMR-deficient cells.[8,9] Undeniably, then, the synthesis and study of small molecules that possess the ability to specifically target DNA defects may afford progress in the development of new cancer diagnostics and therapeutics that are specific for MMR-deficient cancers.

Our laboratory has previously developed a class of compounds, called rhodium metalloinsertors (Figure 1), that target DNA mismatches *in vitro* with high specificity and affinity.[10] The first-generation compound, $[Rh(bpy)_2(chrysi)]^{3+}$ (chrysi = chrysene-5,6-quinonediimine), binds 80% of DNA mismatches in all sequence contexts and preferentially targets thermodynamically destabilized mismatches over matched base pairs by a factor of over 1000.[11] Specifically, it has been shown to bind only at the single mismatch site in a 2725 base-pair plasmid.[12] Additional work focused on incorporating nitrogen atoms into the intercalating ligand in order to increase π-stacking stabilization and led to the development of our second-generation compound, $[Rh(bpy)_2(phzi)]^{3+}$ (phzi = benzo[α]-phenazine-5,6-quinonediimine). This complex exhibits a 50-fold increase in binding affinity compared to $[Rh(bpy)_2(chrysi)]^{3+}$ without a loss in selectivity, allowing for mismatch detection at nanomolar Rh concentrations.[13] The binding mode of these mismatch-specific complexes was determined through the 1.1 Å resolution crystal structure of $[Rh(bpy)_2(chrysi)]^{3+}$ bound to an AC mismatch. The structure revealed the chrysi ligand to insert from the minor groove with ejection of both mismatched bases.[14] NMR studies of $[Rh(bpy)_2(chrysi)]^{3+}$ bound to a CC mismatch further confirmed this binding mode for the complex at mismatched sites in solution.[15] Additional crystal structures of the Rh complex bound to different mismatches[16] as well as structure of a Ru complex bound by insertion to a mismatched site[17] established the generality of metalloinsertion. It is noteworthy that these studies represented the first illustration of the insertion binding mode, proposed originally by L. S. Lerman in the early 1960s.[18]

Received: September 12, 2012
Published: November 8, 2012

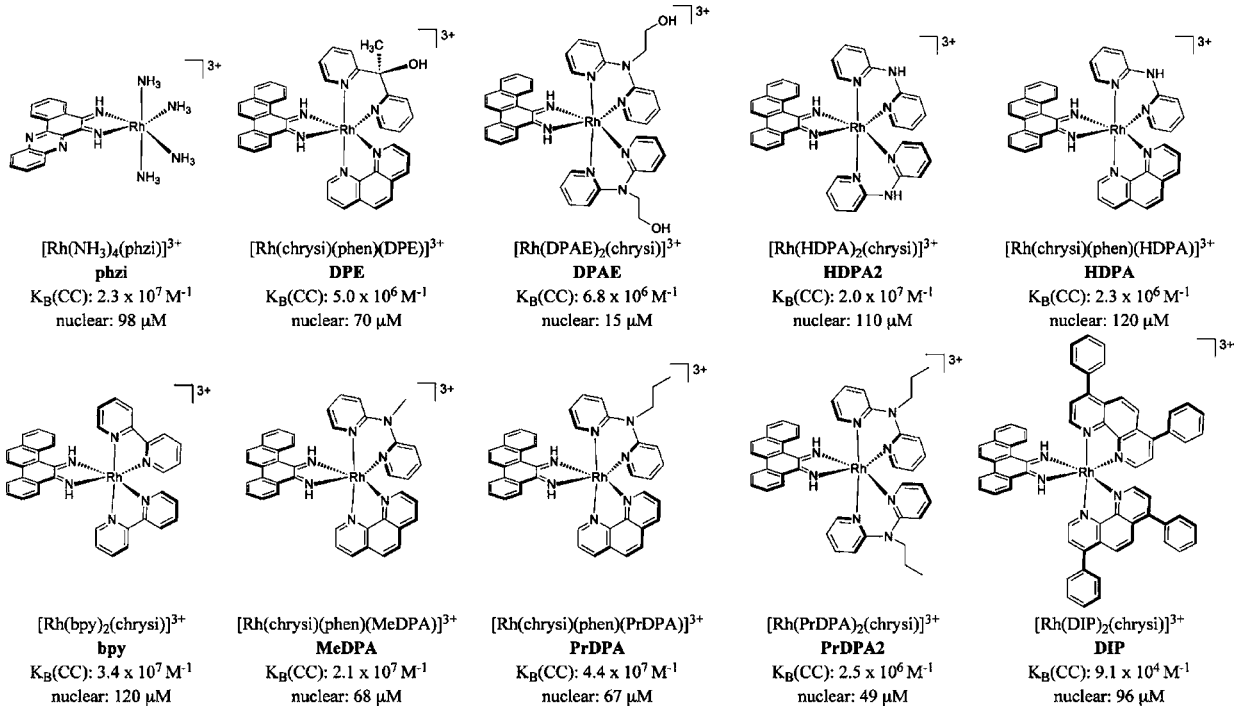

Figure 1. Chemical structures, binding affinities for CC mismatches, and approximated nuclear concentration of all compounds studied. Binding affinities for $[Rh(DIP)_2(chrysi)]^{3+}$, $[Rh(HDPA)_2(chrysi)]^{3+}$, $[Rh(bpy)_2(chrysi)]^{3+}$, $[Rh(DPAE)_2(chrysi)]^{3+}$, and $[Rh(PrDPA)_2(chrysi)]^{3+}$ are previously reported.[10,22,36] Note that all compounds are shown as the 3+ cation; pKa's of the immine protons vary among the complexes and thus the protonation state of the inserting ligand will vary at physiological pH. All other compounds' DNA binding affinities were measured on the 29mer hairpin 5′-GGCAGGCATGGCTTTTTGCCATCCCTGCC-3′ (underline denotes the mismatch) in a competition assay through photocleavage by $[Rh(bpy)_2chrysi]^{3+}$. Samples were irradiated and electrophoresed through a 20% denaturing PAGE gel, and the percent of DNA cleaved at each concentration was plotted as a function of log[Rh]. The data were fitted to a sigmoidal curve, and K_B values were determined by calculating the concentration of rhodium at the inflection points of the curve and solving simultaneous equilibria. To determine nuclear rhodium concentrations, HCT116O cells were incubated in media containing 10 μM of each rhodium complex (except $[Rh(DIP)_2(chrysi)]^{3+}$, which was administered at 2 μM) for 24 h. The cells were harvested by trypsinization and the nuclei isolated. Rhodium content was quantified by ICP-MS first normalized to number of nuclei and then divided by the volume of the nucleus of a HCT116O cell, which was approximated as a sphere with radius 4 μm.[46] It is important to note that, while the structures all illustrate the Δ isomers, all experiments were done with racemic mixtures.

In an effort to characterize the *in cellulo* effects of these metalloinsertors, several cell assay experiments have been undertaken on the isogenic cell lines HCT116N and HCT116O. The HCT116 parent cell line is a human colorectal carcinoma line deficient in the *hMLH*1 gene. This gene encodes for part of the mismatch repair (MMR) machinery; consequently, this cell line is MMR deficient. The HCT116N cell line has been transfected with human chromosome 3 (ch3), which restores MMR proficiency, while the HCT116O cell line has been transfected with human chromosome 2 (ch2), leaving it MMR deficient.[19] These rhodium metalloinsertors have been found selectively to inhibit DNA synthesis in the MMR-deficient HCT116O cell line over the MMR-proficient HCT116N cell line,[20] as measured by an ELISA assay for DNA synthesis.[21] Significantly, the binding affinities of the metalloinsertors were found to correlate directly with the selectivity of the rhodium complexes for the MMR-deficient cell line, lending credence to the idea that these complexes target DNA mismatches *in cellulo* as well as in the test tube.[22]

Recently, it was discovered that the rhodium metalloinsertors that display activity at relatively short incubation times in the ELISA assay also show preferential cytotoxicity toward the MMR-deficient HCT116O cell line, inducing death *via* a necrotic pathway.[23] As one generally accepted trigger of necrosis is severe ATP depletion,[24,25] this observation prompted the investigation of subcellular localization. These metalloinsertors may trigger necrosis through mitochondrial DNA targeting. As lipophilic cations, mitochondrial accumulation is a possibility;[26] real-time monitoring of the cells with confocal microscopy could not be used to monitor organelle accumulation, however, since the rhodium complexes are not luminescent. Nonetheless, an understanding of the subcellular localization of these compounds is crucial for the development of next-generation metalloinsertors with improved selectivity for MMR-deficient cells.[27] Rhodium uptake can be easily probed by inductively coupled plasma mass spectrometry (ICP-MS), as no interfering ion exists within the cell. The sensitivity of ICP-MS allows for biologically relevant concentrations of rhodium to be determined,[28] and combined with organelle isolation procedures, ICP-MS can be used to estimate the subcellular localization of our metalloinsertors.

There have been few studies to date investigating the subcellular localization of common therapeutic agents. Non-fluorescent organic molecules pose a particular problem in this regard owing to their lack of spectroscopic handle for detection unless the drug is tethered to a fluorescent tag. However, this process of appending a fluorescent molecule to a drug has been shown in itself to alter the subcellular localization of the compound.[29] There have been instances where appending an organelle-specific peptide to a therapeutic agent resulted in drastically altered activity of the agent, which was attributed to altered subcellular localization.[30,31] Fluorescent organic ther-

apeutics, as well as metal-based therapeutics, do contain spectroscopic or spectrometric handles for detection, and can therefore be mapped within the cell. Doxorubicin, a chemotherapeutic that intercalates DNA, is one such fluorescent molecule. In one study, doxorubicin resistance was correlated with subcellular localization of the compound. Specifically, the subcellular distribution of the drug shifted from nuclear to cytosolic as drug resistance increased.[32] Furthermore, in a study by Liu and co-workers on a series of Au(I)- and Ag(I)-bidentate pyridyl phosphine anticancer agents, it was observed that increased lipophilicity resulted in increased potency of the drug, with preferential accumulation of the drug in the mitochondria.[33] In a final study, ICP-MS was used to track the uptake and subcellular localization of cisplatin as well as two ruthenium-based chemotherapeutics currently in clinical trials, NAMI-A and KP1019. Reduced mitochondrial accumulation of cisplatin was observed in cisplatin-resistant cells, while the ruthenium-based drugs were found to have different localization patterns than cisplatin which did not change from one cell type to the other.[34]

Here we correlate the selectivity of a variety of rhodium metallointercalators that target MMR-deficient cells with the subcellular localization of the complexes. We find that all complexes studied are localized at a sufficient concentration in the nucleus for mismatch binding. Furthermore, we find that, in general, higher levels of mitochondrial rhodium reduce the cell-selective biological activity of these metallointercalators. These observations give credence to the theory that mismatches in genomic DNA are the ultimate target of our metallointercalators and that this mismatch targeting is responsible for their unique cell-selective biological activity.

EXPERIMENTAL SECTION

Materials. Commercially available chemicals were used as received. The Rh complex $[Rh(NH_3)_5Cl]Cl_2$ was obtained from Strem Chemical, Inc. $RhCl_3$ was purchased from Pressure Chemical, Inc. All organic reagents and Sephadex ion-exchange resin were obtained from Sigma-Aldrich unless otherwise noted. Sep-pak C_{18} solid-phase extraction (SPE) cartridges were purchased from Waters Chemical Co. (Milford, MA). Media and supplements were purchased from Invitrogen (Carlsbad, CA). BrdU, antibodies, buffers, peroxidase substrate, MTT, and acidified lysis buffer (10% SDS in 10 mM HCl) solution were purchased in kit format from Roche Molecular biochemical (Mannheim, Germany). Phosphoramidites were purchased from Glen Research (Sterling, VA).

Oligonucleotide Synthesis. Oligonucleotides were synthesized on an Applied Biosystems 3400 DNA synthesizer using standard phosphoramidite chemistry. DNA was synthesized with a 5′-dimethoxytrityl (DMT) protecting group. The oligonucleotides were cleaved from the beads by reaction with concentrated ammonium hydroxide at 60 °C overnight. The resulting free oligonucleotides were purified by HPLC using a C_{18} reverse-phase column (Varian, Inc.) on a Hewlett-Packard 1100 HPLC. The DMT group was removed by reaction with 80% acetic acid for 15 min at ambient temperature. The DMT-free oligonucleotides were precipitated with absolute ethanol and purified again by HPLC. Positive identification of the oligonucleotides and their purity were confirmed by MALDI-TOF mass spectrometry. Quantification was performed on a Beckman DU 7400 spectrophotometer using the extinction coefficients at 260 nm (ε_{260}) estimated for single-stranded DNA.

Synthesis and Characterization of Metal Complexes. The complexes $[Rh(bpy)_2(chrysi)]^{3+}$, $[Rh(HDPA)_2(chrysi)]^{3+}$, $[Rh(NH_3)_4(chrysi)]^{3+}$, $[Rh(DIP)_2(chrysi)]^{3}$, $[Rh(DPAE)_2(chrysi)]^{3+}$, and $[Rh(PrDPA)_2(chrysi)]^{3+}$ were prepared according to published procedures.[22,35,36] $[Rh(chrysi)(phen)(NH_3)_2]Cl_3$ was prepared from $[Rh(phen)(NH_3)_4]OTf_3$ and 5,6-chrysenequinone following the methods described by Mürner et al.[37] The ligand 1,1-di(pyridin-2-yl)ethanol (DPE) was synthesized according to published procedures.[38]

***N*-Alkyl-*N*-(pyridin-2-yl)pyridin-2-amine (alkyl = methyl or propyl; MeDPA, PrDPA).** To a slurry of sodium hydride (70 mg, 2.9 mmol) in THF (10 mL) was added HDPA (500 mg, 2.9 mmol) in 5 mL THF at 0 °C under 1 atm Ar. The reaction was purged with argon for 15 min, and the appropriate 1-bromoalkane (3.8 mmol) was added dropwise and warmed to ambient temperature. The reaction was stirred an additional 18 h under argon at reflux temperature. The reaction mixture was extracted with dilute sodium bicarbonate, and the aqueous phase was extracted with CH_2Cl_2 (3 × 40 mL). The organic fractions were combined and dried over magnesium sulfate, and the solvent was removed *in vacuo*. These ligands were purified via flash chromatography (SiO_2, 1:9 EtOAc:hexanes).

MeDPA: Yield: 23%. ^{1}H NMR ($CDCl_3$, 300 MHz): δ 8.35 (d of d, 2H); 7.54 (t, 2H); 7.17 (d, 2H); 6.86 (t, 2H), 3.62 (s, 3H). ESI-MS (cation): m/z calc 186.1 ($M + H^+$), obs. 186.

PrDPA: Yield: 25%. ^{1}H NMR ($CDCl_3$, 300 MHz): δ 8.34 (d, J = 7.7 Hz, 2H), 7.57−7.45 (m, 2H), 7.06 (d, J = 0.7 Hz, 2H), 6.90−6.79 (m, 2H), 4.19−4.07 (m, 2H), 1.79−1.65 (m, 2H), 0.99−0.85 (m, 3H). ESI-MS (cation): m/z calc 214.1 ($M + H^+$), obs. 214.

$[Rh(NH_3)_4(phzi)]Cl_3$. $[Rh(NH_3)_6][OTf]_3$ (0.50 g, 0.77 mmol) and benzo[α]phenazine-5,6-dione (0.200 g, 0.77 mmol) were dissolved in a 1:5 mixture of water/acetonitrile (500 mL). A 1 M solution of NaOH (1 mL) was added to the yellow solution and the reaction was allowed to stir at ambient temperature for 45 min, at which time a 1 M solution of HCl (1 mL) was added to neutralize the reaction mixture. The acetonitrile was evaporated *in vacuo*, and the resulting yellow solution was loaded onto a SPE cartridge, eluted with 25% acetonitrile in 0.1% $TFA_{(aq)}$, and lyophilized to give a yellow solid. The chloride salt can be obtained from a Sephadex QAE anion-exchange column equilibrated with 0.1 M $MgCl_2$. Yield: 0.45 g, 76%. ^{1}H NMR (300 MHz, d_6-DMSO): δ 3.79 (s, 6H), 4.48 (d, J = 20.1 Hz, 6 H), 7.92−8.21 (m, 4H), 8.34 (m, 2H), 8.62 (d, J = 7.6 Hz, 1H), 8.96 (d, J = 7.8 Hz, 1 H), 13.88 (s, 1H), 13.98 (s, 1H). ESI-MS (cation): m/z calc 524.07 ($M - NH_3 + TFA^+$), obs. 523.8. UV−vis (H_2O, pH 7): 250 nm (36,800 M^{-1} cm^{-1}), 310 nm (20,800 M^{-1} cm^{-1}), 340 nm (23,400 M^{-1} cm^{-1}).

$[Rh(chrysi)(phen)(L)]Cl_3$. *(L = HDPA, MeDPA, PrDPA,).* $Rh(chrysi)(phen)(NH_3)_2]Cl_3$ (25 mg, 0.02 mmol) was reacted with L (0.022 mmol) in a 4:1 mixture of ethanol/water (10 mL). The bright-red solution was refluxed overnight. The solvent was removed *in vacuo* and the resulting red solid dissolved in 0.1% $TFA_{(aq)}$(10 mL). The red solution was loaded onto a SPE cartridge and rinsed with a copious amount of 0.1% $TFA_{(aq)}$. The SPE cartridge was eluted with 10% acetonitrile in 0.1% $TFA_{(aq)}$, and fractions were collected. The fractions containing product were identified by HPLC, combined, and lyophilized. The chloride salt can be obtained from a Sephadex QAE anion-exchange column equilibrated with 0.1 M $MgCl_2$.

$[Rh(chrysi)(phen)(HDPA)]Cl_3$: Yield: 28%. ESI-MS (cation): m/z calc 708.14 ($M - 2H^+$), obs. 708.2. UV−vis (H_2O, pH 7): 303 nm (34,200 M^{-1} cm^{-1}), 391 nm (8,000 M^{-1} cm^{-1}), 440 nm (3,600 M^{-1} cm^{-1}).

$[Rh(chrysi)(phen)(MeDPA)]Cl_3$: Yield 32%. ESI-MS (cation): m/z calc 722.15 ($M - 2H^+$) 361.6 ($M - H^{2+}$), obs. 722, 362. UV−vis (H_2O, pH 7): 303 nm (55,500 M^{-1} cm^{-1}), 391 nm (13,800 M^{-1} cm^{-1}), 440 nm (5,700 M^{-1} cm^{-1}).

$[Rh(chrysi)(phen)(PrDPA)]Cl_3$: Yield: 22%. ESI-MS: calc 750.18 ($M - 2H^+$), 375.6 ($M - H^{2+}$), obs. 750, 376. UV−vis (H_2O, pH 7): 303 nm (53,500 M^{-1} cm^{-1}), 391 nm (13,900 M^{-1}, cm^{-1}), 440 nm (9,900 M^{-1}, cm^{-1}).

$[Rh(chrysi)(phen)(DPE)]Cl_3$. A 125 mL round-bottomed flask was charged with $[Rh(chrysi)(phen)(NH_3)_2]TFA_3$ (62.0 mg, 0.068 mmol) and DPE (25.6 mg, 0.128 mmol) in ethanol (50 mL) to give a red solution. The reaction was heated to reflux (80 °C) and stirred for 48 h. The ethanol solution was evaporated to dryness and dissolved in 0.1% $TFA_{(aq)}$(50 mL). The red solution was loaded onto a SPE cartridge and rinsed with copious amounts of 0.1% $TFA_{(aq)}$. The SPE cartridge was eluted with 10% acetonitrile in 0.1% $TFA_{(aq)}$ and

dx.doi.org/10.1021/ja3090687 | J. Am. Chem. Soc. 2012, 134, 19223−19233

fractions were collected. The fractions containing product were identified by HPLC, combined, and lyophilized. The chloride salt can be obtained from a Sephadex QAE anion-exchange column equilibrated with 0.1 M $MgCl_2$. Yield: 17 mg. ESI-MS (cation): m/z calc 737.15 ($M - 2H^+$), 369.1 ($M - H^{2+}$), obs. 737, 369. UV−vis (H_2O, pH 7): 272 nm (102,100 M^{-1} cm^{-1}), 303 nm (35,400 M^{-1} cm^{-1}), 440 nm (10,600 M^{-1} cm^{-1}).

Photocleavage Competition Titrations. The oligonucleotide was ^{32}P-labeled at the 5′-end by incubating DNA with ^{32}P-ATP and polynucleotide kinase (PNK) at 37 °C for 2 h, followed by purification using gel electrophoresis. A small amount of the labeled DNA (less than 1% of the total amount of DNA) was added to 2 μM DNA in 100 mM NaCl, 20 mM NaP_i, pH 7.1 buffer. The DNA hairpin was annealed by heating at 90 °C for 10 min and cooling slowly to ambient temperature over a period of 2 h. Racemic solutions of nonphotocleaving rhodium complex ranging from nanomolar to micromolar concentration, as well as a 4 μM $[Rh(bpy)_2(chrysi)]^{3+}$ solution were made in Milli-Q water. Annealed 2 μM DNA (10 μL), 4 μM $[Rh(bpy)_2(chrysi)]^{3+}$ (5 μL), and 5 μL of nonphotocleaving Rh solution at each concentration were mixed in a microcentrifuge tube and incubated at 37 °C for 10 min. A light control (ØRh), in which the DNA was mixed with 10 μL of water and irradiated, and a dark control ($Øh\nu$), in which the DNA was mixed with the highest concentration of rhodium complex without irradiation, were also prepared. The samples were then irradiated on an Oriel (Darmstadt, Germany) 1000-W Hg/Xe solar simulator (340−440 nm) for 5 min. The irradiated samples were dried and electrophoresed in a 20% denaturing polyacrylamide gel. The gel was then exposed to a phosphor screen, and the relative amounts of DNA in each band were quantitated by phosphorimagery (ImageQuant).

Binding Constant Determination. The fraction of DNA cleaved in each lane on the gel (see Figure S1 in the SI for a typical autoradiogram) was normalized and plotted against the log of the concentration of rhodium complex. At least three photocleavage titrations were carried out for each racemic metal complex. The pooled data were fit to a sigmoidal curve using OriginPro 6.1 (see Figure S2 in the SI). The resulting midpoint value (i.e., the log of [rhodium complex] at the inflection point of the curve) was converted to units of concentration ($[Rh_{50\%}]$). The binding and dissociation constants of the nonphotocleaving complex were calculated by solving simultaneous equlibria involving DNA, $[Rh(bpy)_2(chrysi)]^{3+}$, and the complex in question in Mathematica 6.0.

Cell Culture. HCT116N and HCT116O cells were grown in RPMI medium 1640 supplemented with 10% FBS, 2 mM L-glutamine, 0.1 mM nonessential amino acids, 1 mM sodium pyruvate, 100 units/mL penicillin, 100 μg/mL streptomycin, and 400 μg/mL Geneticin (G418). Cells were grown in tissue culture flasks (Corning Costar, Acton, MA) at 37 °C under 5% CO_2 and humidified atmosphere.

Cellular Proliferation ELISA. HCT116N and HCT116O cells were plated in 96-well plates at 2000 cells/well and allowed 24 h to adhere. The cells were then incubated with rhodium for the concentration and durations specified. For incubations less than 72 h, the Rh-containing media was replaced with fresh media, and the cells were grown for the remainder of the 72 h period. Cells were labeled with BrdU 24 h before analysis. The BrdU incorporation was quantified by antibody assay according to established procedures.[39] Cellular proliferation was expressed as the ratio of the amount of BrdU incorporated by the treated cells to that of the untreated cells.

MTT Cytotoxicity Assay. Cytotoxicity assays were performed as described in the literature.[40] HCT116N and HCT116O cells were plated in 96-well plates at 50,000 cells/well and incubated with rhodium for the durations specified. After rhodium incubation, cells were labeled with MTT for 4 h at 37 °C under 5% CO_2 and humidified atmosphere. The resulting formazan crystals were dissolved with solubilizing reagent purchased from Roche according to the manufacturer's instructions. The dissolved formazan was quantified as the absorbance at 570 nm minus the background absorbance at 690 nm. Percent viability was determined as the ratio of the amount of formazan in the treated cells to that of the untreated cells.

Nuclear Isolation Protocol. Approximately 10 million HCT116N/O cells were harvested from adherent culture by trypsinization, washed with cold PBS, and resuspended in 1 mL hypotonic buffer (20 mM TrisHCl pH 7.4, 10 mM NaCl, 3 mM $MgCl_2$). The resulting suspension was incubated on ice for 15 min; 50 μL of a 10% NP-40 solution was added to the solution and immediately followed by vortexing at the highest setting for 10 s. The solution was then centrifuged at 3000g for 10 min. The supernatant was discarded and the pellet saved as the nuclear fraction.

Mitochondrial Isolation Protocol. The followed protocol is an adaptation of that used by Ahmad et al.[41] Approximately 20 million HCT116N/O cells were harvested from adherent culture by trypsinization, washed with cold PBS, and resuspended in 500 μL of mitochondrial extraction buffer (200 mM mannitol, 68 mM sucrose, 50 mM pipes, 50 mM KCl, 5 mM EGTA, 2 mM $MgCl_2$, 1 mM DTT, protease inhibitors). The resulting suspension was incubated on ice for 20 min and then homogenized by 35 passes through a 21 gauge needle and 1-mL syringe. The resulting lysate was centrifuged at 150g for 5 min. The supernatant was then transferred to a new microcentrifuge tube and centrifuged for an additional 10 min at 14,000g. The supernatant was discarded and the pellet saved as the mitochondrial fraction.

ICP-MS Assay for Whole-Cell Rhodium Levels. HCT116O cells were plated at 1×10^6 cells/well in a 6 well plate. The cells were allowed 24 h to adhere, then treated with 10 μM of rhodium complex. After the appropriate amount of time, the media was decanted, the cell monolayer washed with 3 mL PBS, and the cells lysed with 800 μL of 1% SDS. The cell lysate was further lysed by sonication on a Qsonica Ultrasonic processor for 10 s at 20% amplitude; 750 μL of the lysate was then combined with 750 μL of a 2% HNO_3 (v/v) solution, while the remainder of the lysate was quantified for protein by a bicinchoninic assay (BCA).[42] The 1% HNO_3 solution was analyzed for rhodium content on an HP-4500 ICP-MS unit. Rhodium counts were normalized to the amount of protein determined from the BCA analysis (to obtain ng [rhodium]/mg [protein] values). Standard errors for three independent experiments are shown. The experiment was repeated with HCT116N cells for one time point only to verify similar uptake of rhodium by the two cell lines.

ICP-MS Assay for Nuclear Rhodium Levels. HCT116O cells were plated at 10×10^6 cells/plate in culture flasks and allowed 24 h to adhere. The cells were then treated with 10 μM of rhodium complex (except $[Rh(DIP)_2(chrysi)]^{3+}$, which was administered at 2 μM) for 24 h, harvested by trypsinization, and washed with PBS. The nuclear isolation protocol was then performed on the cells. The resulting pellet was resuspended in 800 μL of Milli-Q water and lysed by sonication on a Qsonica Ultrasonic processor for 10 s at 40% amplitude; 750 μL of the lysate was then combined with 750 μL of a 2% HNO_3 (v/v) solution, while the remainder of the lysate was quantified for protein by a bicinchoninic assay (BCA).[42] The resulting 1% HNO_3 solution was analyzed for rhodium content on an HP-4500 ICP-MS unit. Rhodium counts were normalized to the amount of protein determined from the BCA analysis (to obtain ng [rhodium]/mg [protein]). The protein content was converted to number of nuclei by the conversion factor 3.28×10^{-8} mg [nuclear protein]/nuclei (found by counting nuclei with a hemacytometer followed by lysing and protein quantification). The rhodium concentrations were then divided by nuclei density to obtain ng of rhodium per nucleus. Standard errors for three independent experiments are shown. The experiment was repeated with HCT116N cells to verify similar uptake of rhodium by the two cell lines.

ICP-MS Assay for Mitochondrial Rhodium Levels. HCT116O cells were plated at 15×10^6 cells/plate in culture flasks and allowed 24 h to adhere. The cells were then treated with 10 μM of rhodium complex for 24 h, harvested by trypsinization, and washed with PBS. The mitochondrial isolation protocol was then performed on the cells. The resulting pellet was resuspended in 800 μL of Milli-Q water and lysed by sonication on a Qsonica Ultrasonic processor for 10 s at 40% amplitude; 750 μL of the lysate was then combined with 750 μL of a 2% HNO_3 (v/v) solution, while the remainder of the lysate was quantified for protein by a bicinchoninic assay (BCA). The resulting

1% HNO_3 solution was analyzed for rhodium content on an HP-4500 ICP-MS unit. Rhodium counts were normalized to the amount of protein determined from the BCA analysis (to obtain ng [rhodium]/mg [protein] values). Standard errors for three independent experiments are shown. The experiment was repeated with HCT116N cells for one time point only to verify similar uptake of rhodium by the two cell lines.

RESULTS

Binding Affinities for Metal Complexes at Single Base Mismatches. The binding constants of the various rhodium metalloinsertors at a CC mismatch in a 29-mer DNA hairpin with the sequence 5′-GGCAGGCATGGCTTTTTGCCATCCCTGCC-3′ (underline denotes the mismatch) were measured. The hairpin sequence allows cleavage site determination on either strand around the mismatch site. All newly synthesized rhodium complexes promote relatively little DNA cleavage upon irradiation, and as such their binding affinities were determined through binding competition titrations with 1 μM *rac*-$[Rh(bpy)_2(chrysi)]^{3+}$, which does cleave DNA upon irradiation.[10−12] A representative photocleavage titration can be found in Figure S1 in the SI. The degree of photocleavage can be plotted against the log[Rh] and fit to a sigmoidal curve (See Figure S2 in the SI). On the basis of the binding constant of $[Rh(bpy)_2(chrysi)]^{3+}$, the binding constants of all subsequent complexes are then determined by solving simultaneous equilibria at the inflection point of the photocleavage titration curve. The results, along with those of all previously reported compounds,[22,36] are shown in Figure 1. Interestingly, despite the variance in both the ancillary ligands and number of hydrogen-bond donors, all compounds (except the extremely bulky $[Rh(DIP)_2(chrysi)]^{3+}$) exhibit binding affinities within essentially the same order of magnitude, varying from 2.3×10^6 M^{-1} to 4.4×10^7 M^{-1}.

Quantitation of Inhibition of Cellular Proliferation using an Enzyme-Linked Immunosorbent Assay (ELISA). An ELISA for DNA synthesis was used to quantify the effects of the metalloinsertors on the proliferation of HCT116N cells (MMR-proficient) and HCT116O cells (MMR-deficient). Both cell lines were incubated with 0−25 μM of each compound (except $[Rh(DIP)_2(chrysi)]^{3+}$ and $[Rh(chrysi)(phen)(DPE)]^{3+}$, which were both administered at 0−5 μM concentrations due to increased potency). Incubations were performed for 1, 3, 6, 12, or 24 h. After the incubations, the medium containing Rh was replaced with fresh medium, and the cells were grown for the remainder of the 72 h period. The extent of cellular proliferation is expressed as the ratio of BrdU incorporated by the rhodium-treated cells as compared to untreated controls. Furthermore, we define differential inhibition as the difference in BrdU incorporation between the HCT116N and HCT116O cells. Figure 2 shows representative data for $[Rh(chrysi)(phen)(DPE)]^{3+}$. Data for all other compounds can be found in Figures S3−S12 in the SI. Very little to no activity is seen for any of the compounds at 1 or 3 h incubation times (data not shown).

Figure 3 summarizes the ELISA results for all compounds tested at 10 μM rhodium concentration and 24 h of incubation (except $[Rh(DIP)_2(chrysi)]^{3+}$, which is shown at 2 μM), as these are the same conditions used for all ICP-MS experiments.[22,36,43] There are four compounds with high selectivity for the MMR-deficient HCT116O cells ($[Rh(NH_3)_4(phzi)]^{3+}$, $[Rh(chrysi)(phen)(DPE)]^{3+}$, $[Rh(DPAE)_2(chrysi)]^{3+}$, and $[Rh(HDPA)_2(chrysi)]^{3+}$, all shown in different shades of blue), displaying differential inhibitions of 63 ± 5%, 55 ± 3%, 55 ± 3%, and 52 ± 2%, respectively. $[Rh(chrysi)(phen)(HDPA)]^{3+}$ and $[Rh(bpy)_2(chrysi)]^{3+}$ exhibit modest selectivity with differential inhibitions of 27 ± 2% and 8 ± 2% at 24 h (shown in green in Figure 3). It should be noted that at longer incubation times the differential inhibition of $[Rh(bpy)_2(chrysi)]^{3+}$ increases.[22] $[Rh(chrysi)(phen)(MeDPA)]^{3+}$, also shown in green, exhibits delayed biological activity. At 24 h incubation times, this complex does not display significant inhibition of DNA synthesis toward either cell line. The remaining compounds ($[Rh(chrysi)(phen)(PrDPA)]^{3+}$, $[Rh(PrDPA)_2(chrysi)]^{3+}$, and $[Rh(DIP)_2(chrysi)]^{3+}$, shown in red) exhibit no selectivity for

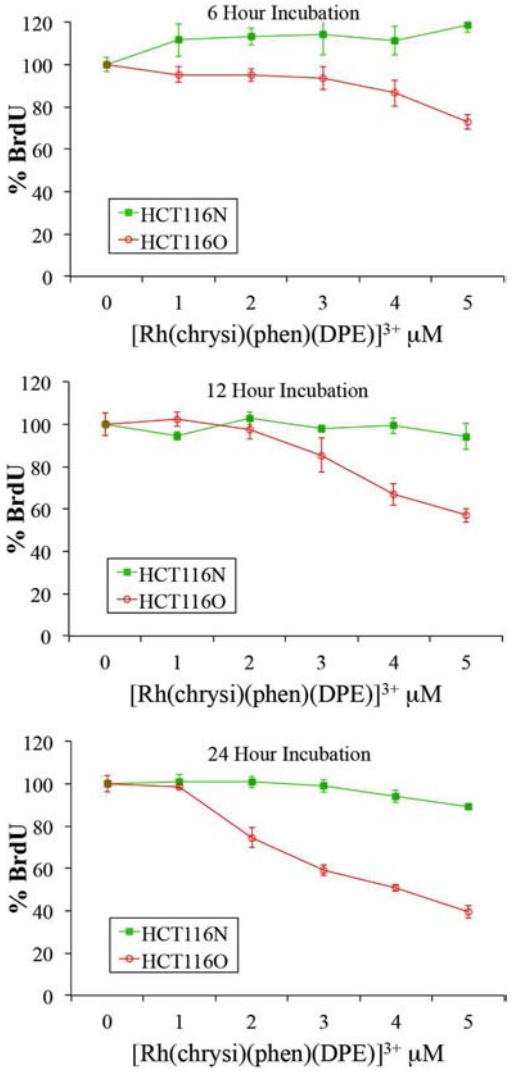

Figure 2. Inhibitory effects of $[Rh(chrysi)(phen)(DPE)]^{3+}$ as a function of incubation time on cellular proliferation. Shown are plots of BrdU incorporation (a measure of DNA synthesis and therefore cellular proliferation) normalized to the BrdU incorporation of untreated cells as a function of rhodium concentration. Standard error bars for five trials are shown. MMR-proficient HCT116N cells (green) and MMR-deficient HCT116O cells (red) were plated and allowed to adhere 24 h before incubation with 0−5 μM for 1, 3, 6, 12, or 24 h. At the end of the incubations, the medium containing rhodium was replaced with fresh medium for the remainder of the 72 h period, followed by ELISA analysis. BrdU was added to the medium 24 h prior to analysis. One hour and 3 h plots are not shown, as no activity was observed.

dx.doi.org/10.1021/ja3090687 | J. Am. Chem. Soc. 2012, 134, 19223−19233

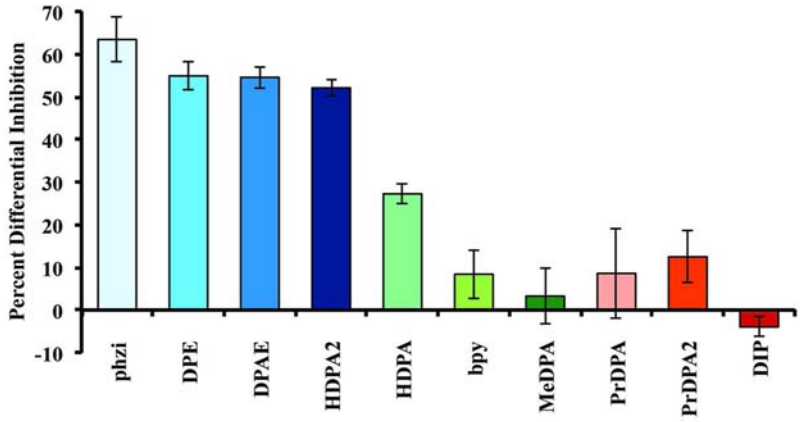

Figure 3. Inhibitory effects of rhodium metalloinsertors as a function of metalloinsertor identity. The percent differential inhibition is defined as the difference of the normalized percentages of cellular proliferation between the two cell lines, HCT116O vs HCT116N. ELISA analyses were performed as in Figure 2. Cells were incubated with 10 μM rhodium complex for 24 h (except $[Rh(DIP)_2(chrysi)]^{3+}$, which was administered at 2 μM).

the MMR-deficient HCT116O cell line, and inhibit DNA synthesis similarly in both cell lines. It should be noted that none of the complexes studied show a differential inhibition favoring the HCT116N cell line, although that is the common result for many DNA damaging agents.

Many of these compounds exhibit accelerated activity in the ELISA assay, displaying substantial differential inhibition of DNA synthesis toward the HCT116O cell line at 6 or 12 h incubation times. Motivated by the previous observation that rhodium metalloinsertors which display accelerated activity in the ELISA assay exhibit preferential cytotoxicity toward the MMR-deficient HCT116O cell line,[23] we chose also to test all compounds for cytotoxicity in the MTT assay.

MTT Cytotoxicity Assay. The cytotoxic effects of all compounds were determined by MTT assay.[40] Briefly, reduction of the MTT reagent by metabolically active cells leads to the production of formazan, which can then be dissolved in acidified SDS to produce a characteristic absorbance at 570 nm. This absorbance reflects the percentage of metabolically active cells in each sample. HCT116N and HCT116O cells were plated and treated with the various rhodium complexes at the concentrations indicated in Figure 4 for 24, 48, or 72 h. Percent viability is defined as the ratio of the amount of formazan in the treated cells to that in the untreated cells, and differential cytotoxicity is defined as the difference between the percent viabilities of the two cell lines. The 72 h results are shown in Figure 4. These results are consistent with the ELISA assay results. The same four compounds that show the best differential inhibition of DNA synthesis in the ELISA assay ($[Rh(NH_3)_4(phzi)]^{3+}$, $[Rh(chrysi)(phen)(DPE)]^{3+}$, $[Rh(DPAE)_2(chrysi)]^{3+}$, and $[Rh(HDPA)_2(chrysi)]^{3+}$) exhibit highly selective cytotoxicities toward the MMR-deficient HCT116O cell line, 72 ± 4%, 69 ± 3%, 47 ± 1%, and 55 ± 1%, respectively (at their respective optimal concentrations). The compounds that exhibit delayed activity in the ELISA assay ($[Rh(chrysi)(phen)(MeDPA)]^{3+}$ and $[Rh(bpy)_2(chrysi)]^{3+}$) do not display significant cytotoxicity toward either cell line in the MTT assay, consistent with previous observations.[23] The remaining compounds ($[Rh(chrysi)(phen)(HDPA)]^{3+}$, $[Rh(chrysi)(phen)(PrDPA)]^{3+}$, $[Rh(PrDPA)_2(chrysi)]^{3+}$, and $[Rh(DIP)_2(chrysi)]^{3+}$) exhibit either modest or no selective cytotoxicity toward the HCT116O cell line, consistent with their activities in the ELISA assay.

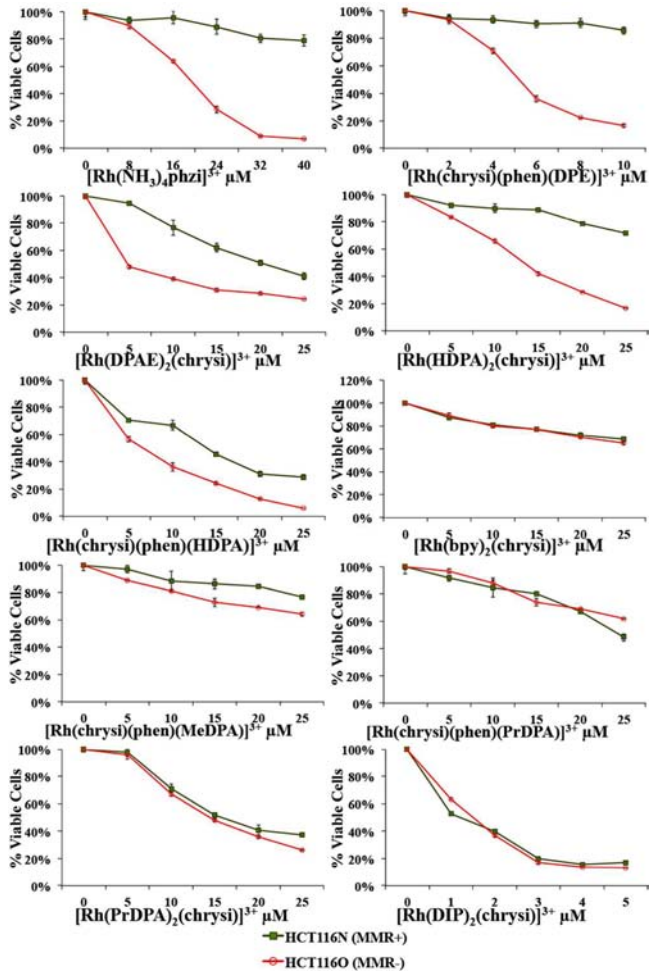

Figure 4. Differential cytotoxicities of rhodium metalloinsertors. HCT116N (green) and HCT116O (red) cells were plated in 96-well format at densities of 5 × 10^4 cells/well and treated with the concentrations of rhodium metalloinsertors indicated. After 72 h, the cells were labeled with MTT for 4 h.

Despite our previous results[22] that rhodium metalloinsertors' biological activity correlates directly with their binding affinities, the metalloinsertors discussed herein have similar DNA binding affinities (except $[Rh(DIP)_2(chrysi)]^{3+}$), yet display biological

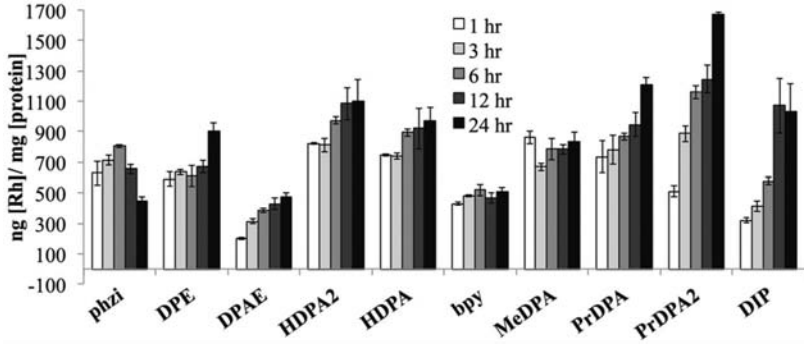

Figure 5. ICP-MS assay for whole-cell rhodium accumulation. HCT116O cells were treated with 10 μM of each rhodium complex (except $[Rh(DIP)_2(chrysi)]^{3+}$, which was administered at 2 μM) for 1, 3, 6, 12, or 24 h. The cells were analyzed for rhodium content by ICP-MS. The rhodium counts were normalized to protein content, which was determined by a BCA assay. See the Experimental Section.

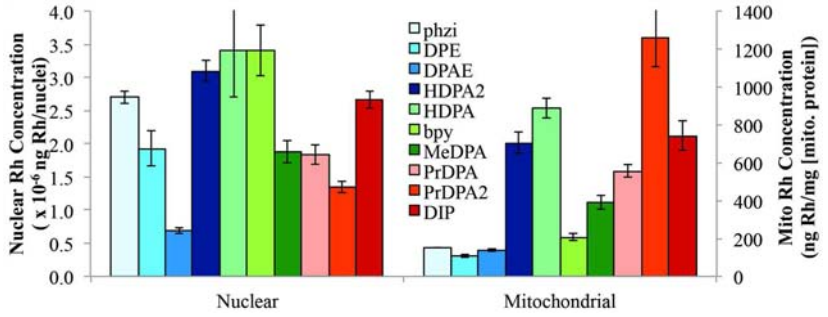

Figure 6. ICP-MS assay for nuclear and mitochondrial rhodium accumulation. HCT116O cells were treated with 10 μM of each rhodium complex (except $[Rh(DIP)_2(chrysi)]^{3+}$, which was administered at 2 μM) for 24 h. The cells were harvested by trypsinization and appropriate organelle isolation procedures performed. The mitochondrial rhodium counts were normalized to protein content, which was determined by a BCA assay. The nuclear rhodium numbers were normalized to number of nuclei.

activities that vary drastically. ICP-MS studies were undertaken in order to determine if the cellular uptake and distribution of these rhodium metalloinsertors could explain their variation in activities.

ICP-MS Assay for Whole-Cell Rhodium Levels. HCT116O cells were treated with 10 μM of each rhodium complex (except $[Rh(DIP)_2(chrysi)]^{3+}$, which was administered at 2 μM) for 1, 3, 6, 12, or 24 h. Whole cell lysates were analyzed for rhodium levels by ICP-MS and normalized to protein content (Figure 5). The experiment was repeated with HCT116N cells at 24 h to confirm that cellular uptake is not different for the HCT116 O versus N cells and to verify consistency in trends among the 10 compounds.

There seems to be a variety of modes of uptake at play. The most lipophilic compounds, $[Rh(chrysi)(phen)(PrDPA)]^{3+}$, $[Rh(PrDPA)_2(chrysi)]^{3+}$, and $[Rh(DIP)_2(chrysi)]^{3+}$, exhibit a gradual uptake into the HCT116O cells, suggestive of passive diffusion. This is consistent with previous studies conducted on luminescent $[Ru(L)_2dppz]^{2+}$ (dppz = dipyrido[3,2-α:2′,3′-c]phenazine) analogues, demonstrating cellular accumulation through passive diffusion, facilitated by the negative potential difference across the cell membrane.[44,45] The two compounds that exhibit delayed biological activity in the ELISA assay ($[Rh(chrysi)(phen)(MeDPA)]^{3+}$ and $[Rh(bpy)_2(chrysi)]^{3+}$) exhibit no increase in cellular rhodium levels after initial uptake at 1 h. Furthermore, the two compounds with HDPA ligands exhibit an enhanced cellular uptake despite reduced lipophilicities. They show a very high initial uptake, followed by a slight increase over the next 23 h. The MeDPA compound does not exhibit the increase in uptake that we had expected, given its enhanced lipophilicity compared to the HDPA analogue. This suggests a completely different mechanism of uptake for the HDPA complex. The two compounds with PrDPA ligands do exhibit enhanced uptakes compared to their respective HDPA analogues at 24 h, but not nearly to the degree we would have expected based on lipophilicities. However, both the PrDPA compounds appear to be taken up through passive diffusion, unlike the HDPA compounds. Perhaps the fact that the HDPA ligand has the potential to form hydrogen bonds *in cellulo* is important to its path into the cell. The compounds that exhibit the highest selectivities in the biological assays ($[Rh(chrysi)(phen)(DPE)]^{3+}$, $[Rh(DPAE)_2(chrysi)]^{3+}$, and $[Rh(NH_3)_4(phzi)]^{3+}$) by no means have the highest overall rhodium levels. In fact, all three of them have among the lowest amount of rhodium uptake into cells.

ICP-MS Assay for Nuclear Rhodium Levels. The nuclear rhodium concentrations of all compounds were determined via ICP-MS. Briefly, HCT116O cells were treated with the various rhodium complexes for 24 h, the nuclei were isolated, and rhodium concentrations of the various samples were determined by ICP-MS and normalized to number of nuclei. The process was repeated with HCT116N cells to confirm that the two cell lines behave similarly and to verify consistency in trends among the 10 compounds (data not shown). These numbers (in nanograms of rhodium per nuclei) can be used to estimate nuclear concentrations by approximating the nucleus of a HCT116O cell as a sphere with radius 4 μm.[46] The approximate nuclear rhodium concentrations, so determined, are reported in Figure 1.

dx.doi.org/10.1021/ja3090687 | J. Am. Chem. Soc. 2012, 134, 19223−19233

As can be seen in Figure 6, there is little correlation between cell-selective activity and nuclear rhodium concentration. In fact, all nuclear rhodium concentrations except for that of $[Rh(DPAE)_2(chrysi)]^{3+}$ are within a factor of 2 of each other and hardly vary among the 10 compounds. When we approximate the nuclear concentrations in molarity of the 10 compounds, all compounds are present in the nucleus at concentrations on the order of 10^{-5} to 10^{-4} M. These concentrations are all more than 2 orders of magnitude higher than the binding affinities for *in vitro* mismatch detection (yet below nonspecific DNA binding levels). Thus even estimating the error on these numbers to be an order of magnitude, all compounds are present in the nucleus at concentrations sufficient for mismatch binding.

ICP-MS Assay for Mitochondrial Rhodium Levels. The mitochondrial rhodium concentrations of all compounds were determined via ICP-MS. Briefly, HCT116O cells were treated with the various rhodium complexes for 24 h, the mitochondria were isolated, and rhodium concentrations of the various samples were determined by ICP-MS and normalized to amount of protein. The results are summarized in Figure 6 alongside the nuclear rhodium levels. The fact that the three compounds with the most cell-selective biological activity ($[Rh(NH_3)_4(phzi)]^{3+}$, $[Rh(chrysi)(phen)(DPE)]^{3+}$, and $[Rh(DPAE)_2(chrysi)]^{3+}$, shown in blue) have the lowest mitochondrial rhodium accumulation, 152 ± 3 ng [Rh]/ mg [mitochondrial protein], 106 ± 7 ng [Rh]/ mg [mitochondrial protein], and 141 ± 8 ng [Rh]/ mg [mitochondrial protein], respectively, is striking. This correlation indicates that the biological target of our rhodium metalloinsertors is genomic DNA rather than mitochondrial DNA.

Furthermore, the three compounds that exhibit no selectivity for the MMR-deficient HCT116O cell line in both biological assays ($[Rh(chrysi)(phen)(PrDPA)]^{3+}$, $[Rh(PrDPA)_2(chrysi)]^{3+}$, and $[Rh(DIP)_2(chrysi)]^{3+}$, shown in red) display the highest levels of mitochondrial rhodium accumulation, 560 ± 30 ng [Rh]/ mg [mitochondrial protein], 1260 ± 150 ng [Rh]/ mg [mitochondrial protein] and 740 ± 70 ng [Rh]/ mg [mitochondrial protein], respectively. This result points to mitochondrial targeting as responsible for the promiscuous biological activity associated with these three compounds that detracts from the cell-selective activity. The two HDPA-containing compounds stray from the trends observed with the other eight compounds.

DISCUSSION

Variations in Complexes Synthesized. The compounds displayed in Figure 1 were synthesized initially in order to investigate the biological effects of varying the lipophilicity of the metalloinsertor. $[Rh(HDPA)_2(chrysi)]^{3+}$ has been shown to exhibit accelerated biological activity, as well as an enhanced selectivity for the MMR-deficient HCT116O cell line compared to that expected based solely on its binding affinity.[22,23] By varying L in $[Rh(chrysi)(phen)(L)]^{3+}$ from HDPA to MeDPA to PrDPA, we sought to examine the effect that changes in lipophilicity have on uptake and to determine if the proton associated with the HDPA ligand, which is not present in other compounds examined, might play some role in the enhanced activity and uptake of $[Rh(HDPA)_2(chrysi)]^{3+}$. The DPE ligand is an analogue of HDPA, but without the amine nitrogen which is capable of inverting its geometry. This therefore affords an analogue of $[Rh(chrysi)(phen)(HDPA)]^{3+}$ with a less flexible dipyridyl ligand that still has the potential to form hydrogen bonds. The chrysi analogue of $[Rh(NH_3)_4(phzi)]^{3+}$ was shown to exhibit excellent differential activity in the ELISA assay,[22] and therefore its phzi analogue was synthesized both in the hopes of making a compound with increased efficacy[13] and to look at the biological effects of decreasing lipophilicity. The compounds $[Rh(DPAE)_2(chrysi)]^{3+}$ and $[Rh(PrDPA)_2(chrysi)]^{3+}$ were made as a matched pair to look at the biological effects of small structural changes to the ancillary ligands.

Surprisingly, all compounds exhibited binding affinities within the same order of magnitude (except $[Rh(DIP)_2(chrysi)]^{3+}$, which was included in the study as a reference compound with extreme lipophilicity, poor binding to mismatches, and no selectivity in our biological assays). The differences among these nine compounds in the ELISA and MTT assays therefore arise from primarily biological effects rather than mismatch binding.

For all compounds, the cytotoxic effects seen in the MTT assay reflect the antiproliferative activity seen in the ELISA assay. Both compounds that exhibit delayed activity in the ELISA assay, $[Rh(chrysi)(phen)(MeDPA)]^{3+}$ and $[Rh(bpy)_2(chrysi)]^{3+}$, do not show any significant cytotoxicity in the MTT assay. Furthermore, the four compounds with the largest differential inhibitions in the ELISA assay, $[Rh(NH_3)_4(phzi)]^{3+}$, $[Rh(chrysi)(phen)(DPE)]^{3+}$, $[Rh(DPAE)_2(chrysi)]^{3+}$, and $[Rh(HDPA)_2(chrysi)]^{3+}$, also show the largest differential cytotoxicities by the MTT assay. Finally, the three compounds with no differential activity in the ELISA assay, $[Rh(chrysi)(phen)(PrDPA)]^{3+}$, $[Rh(PrDPA)_2(chrysi)]^{3+}$, and $[Rh(DIP)_2(chrysi)]^{3+}$, also show no differential cytotoxicity in the MTT assay. It is important to distinguish the absence of differential activity, where the compound shows no selectivity for one cell line over the other and affects both cell lines to the same degree, versus the absence of all activity, where the compound shows no appreciable biological effect on either cell line.

Significantly, the biological activities of these compounds vary dramatically despite their similar binding affinities. Interestingly, the effect of appending a lipophilic alkyl chain to the back of the HDPA ligand either significantly slows down all activity, as with the MeDPA derivative, or instead abolishes the selectivity of the compound for the MMR-deficient HCT116O cell line, as with the PrDPA derivatives. While the mechanism of inhibition is not yet fully understood, one possible scenario is protein recognition of the metalloinsertor-mismatch complex, generating a covalent protein−DNA lesion. Bulky tethers off the back of the metalloinsertor may inhibit the formation of such a lesion, leading to the aforementioned observations. Yet another explanation for the results might be that the increased lipophilicity of the metalloinsertor enhances uptake into the cell but also alters the subcellular localization of the complex once it has entered the cell. This altered subcellular localization could be the reason for the lack of selectivity of the compound for one cell line over the other. Indeed, the least lipophilic compounds have the most selective biological activity, while the more lipophilic compounds exhibit no selective biological activity.

Metalloinsertor Uptake and Nuclear Accumulation. Table 1 displays qualitative nuclear and mitochondrial uptake properties, as well as the presence or absence of cell-selective biological activity for all 10 metalloinsertors. Importantly, the biological effects seen in both assays can be explained by the subcellular localization of the metalloinsertors. If passive

dx.doi.org/10.1021/ja3090687 | J. Am. Chem. Soc. 2012, 134, 19223−19233

Table 1. Qualitative Nuclear[a] and Mitochondrial[b] Uptake Properties, As Well As the Presence or Absence of Cell-Selective Biological Activity[c] for All 10 Metalloinsertors

cmpd	nuclear concn[a]	mito. concn[b]	cell-selective activity[c]
$[Rh(NH_3)_4(phzi)]^{3+}$	+	−	+
$[Rh(chrysi)(phen)(DPE)]^{3+}$	+	−	+
$[Rh(DPAE)_2(chrysi)]^{3+}$	+	−	+
$[Rh(HDPA)_2(chrysi)]^{3+}$	+	+	+
$[Rh(chrysi)(phen)(HDPA)]^{3+}$	+	+	+
$[Rh(bpy)_2(chrysi)]^{3+}$	+	+	−
$[Rh(chrysi)(phen)(MeDPA)]^{3+}$	+	+	−
$[Rh(chrysi)(phen)(PrDPA)]^{3+}$	+	+	−
$[Rh(PrDPA)_2(chrysi)]^{3+}$	+	+	−
$[Rh(DIP)_2(chrysi)]^{3+}$	+	+	−

[a]Compound is considered to have "+" nuclear concentration if its nuclear concentration is sufficient for mismatch detection given its binding affinity. [b]Compound is considered to have "+" mitochondrial concentration if its mitochondrial rhodium concentration is ≥200 ng Rh/mg [mito protein]. [c]Compound is considered to have "+" cell-selective activity if its differential inhibition of DNA synthesis as measured by ELISA of the MMR proficient line vs the MMR-deficient line is ≥25% at 24 h of incubation, 10 μM compound concentration.

diffusion were the dominant mode of cellular uptake for these metalloinsertors,[44,45] the more lipophilic compounds would be expected to have increased cellular uptake. And indeed, except for the HDPA compounds, the most lipophilic compounds do exhibit the greatest cellular accumulation. However, the more liphophilic compounds are in general associated with little differential biological activity; high accumulations of these metalloinsertors are toxic.

By altering L in $[Rh(chrysi)(phen)(L)]^{3+}$ from HDPA to MeDPA to PrDPA, we do not observe an increase in uptake. In fact, the HDPA complex seems to show enhanced uptake in comparison with those that are more lipophilic. Furthermore, both compounds that possess HDPA ligands display both enhanced and accelerated uptake. This is likely due to additional uptake pathways facilitating the influx of complexes containing HDPA. Indeed, several bis(cyclometalated) iridium(III) polypyridine complexes have been shown to employ more than one mechanism of uptake,[47] and this may be the case for several of our metalloinsertors. In comparing $[Rh(PrDPA)_2(chrysi)]^{3+}$ to $[Rh(DPAE)_2(chrysi)]^{3+}$, it appears that by altering the methyl group of PrDPA to an alcohol, uptake is decreased by a factor of 4, yet only the DPAE compound has cell-selective activity. Lastly, the most polar compound, $[Rh(NH_3)_4(phzi)]^{3+}$, displays a peak in uptake at 3 h, after which cellular rhodium levels seem to decrease steadily. This is most likely caused by an efflux mechanism, that is, pumping the complex out of the cell. The ATP-binding cassette protein ABCG2 has been reported to be overexpressed in HCT116 cells,[48] is known to exhibit substrate promiscuity,[49] and may be responsible. Contrary to what would be expected, three of the four compounds with high activity have among the lowest cellular uptake at 24 h, while the three compounds with no cell-selective activity have among the highest cellular uptake at 24 h. It appears as though increased cellular uptake is actually detrimental to the unique cell-selective behavior of our metalloinsertors.

Significantly, the nuclear rhodium concentrations vary only slightly among the 10 compounds. Importantly, by approximating the nucleus of an HCT116O cell as a sphere with diameter 8 μm,[46] all of our metalloinsertors are present in the nucleus at sufficient concentrations for mismatch binding, given their *in vitro* binding affinities (See Figure 1). Moreover, all metalloinsertors are below nonspecific DNA binding concentrations, which precludes nonspecific DNA binding as a possible cause of the nonselective toxicity seen with 3 of our metalloinsertors. The only difference between the two cell lines is the presence of a functional copy of the MLH1 gene in the HCT116N cell line, which encodes for a MMR protein found in the nucleus.[50] Therefore, any interactions the rhodium complexes have with the cell that are not associated with the nucleus may account for their nonspecific biological activity. Consequently, if nuclear DNA were the only cellular target for these metalloinsertors, then all compounds should exhibit similar differential activity due to their similar nuclear concentrations. However, these metalloinsertors could also interact with mitochondrial DNA, or become sequestered in lipid membranes throughout the cell (including the nuclear membrane, which would cause the nuclear rhodium concentration of such a complex to appear higher than it actually is), both of which would result in nonspecific biological activity.

Mitochondrial Accumulation of Rhodium Metalloinsertors. Importantly, the metalloinsertors that display highly cell-selective biological activity are generally associated with lower mitochondrial rhodium accumulation (Figure 6, complexes shown in blue), while the metalloinsertors that display nonselective toxicity show larger mitochondrial rhodium accumulation (Figure 6, complexes shown in red). These observations suggest that it is nuclear DNA targeting of our metalloinsertors that is responsible for their cell-selective biological activities rather than mitochondrial DNA targeting.

The two compounds $[Rh(DPAE)_2(chrysi)]^{3+}$ and $[Rh(PrDPA)_2(chrysi)]^{3+}$ exhibit this phenomenon quite simply.[36] The only structural difference between the two compounds is the substitution of the methyl group of the PrDPA ligand for a primary alcohol in the DPAE ligand. While this substitution is structurally minute, the consequences of such a substitution are extreme from a biological standpoint. This substitution causes a large increase in polarity for the DPAE complex, as can be quantified by a decrease in the logP values from −1.0 to −1.5.[36] Significantly, this increase in polarity is accompanied by an increase in cell-selective biological activity. While the more lipophilic $[Rh(PrDPA)_2(chrysi)]^{3+}$ complex exhibits no selectivity for the MMR-deficient cell line, the more polar $[Rh(DPAE)_2(chrysi)]^{3+}$ complex is highly selective for the MMR-deficient line over the MMR-proficient line. Furthermore, this small structural change results in dramatic changes in uptake and localization of the compounds. While the more lipophilic $[Rh(PrDPA)_2(chrysi)]^{3+}$ complex has about a 4-fold greater uptake into the cell than the polar $[Rh(DPAE)_2(chrysi)]^{3+}$ complex, it exhibits a 10-fold greater mitochondrial accumulation than the DPAE complex, and only a 2-fold greater nuclear accumulation. This suggests that the nonselective behavior of $[Rh(PrDPA)_2(chrysi)]^{3+}$ is caused by increased mitochondrial accumulation.

It should be noted, however, that mitochondrial accumulation is not always associated with nonselective toxicity. The presence of the HDPA ligand enhances and accelerates uptake significantly, and even leads to increased mitochondrial accumulation, yet complexes containing HDPA show highly selective biological activitites. In fact, it has recently been reported that changes in polarity can affect whether

dx.doi.org/10.1021/ja3090687 | J. Am. Chem. Soc. 2012, 134, 19223−19233

mitochondria-targeted peptides simply accumulate in the mitochondrial matrix or disrupt the mitochondrial membrane activity and result in apoptosis.[51] Furthermore, while the antimetabolite methotrexate normally exhibits toxicity toward mammalian cells, when it is conjugated to a mitochondrial-penetrating peptide, the altered subcellular localization reduces its toxicity by 3 orders of magnitude.[30]

General Implications for Design. This work supports the hypothesis that nuclear DNA mismatch binding is responsible for the unique cell-selective biological activity of our rhodium metalloinsertors. Indeed, out of 10 compounds studied, all 10 exhibit sufficient nuclear uptake for mismatch binding. Furthermore, the fact that the three compounds that are not selective for the MMR-deficient cell line have enhanced mitochondrial accumulation indicates that mitochondrial mismatch DNA targeting is not responsible for cell-selective behavior. As the only difference between the two cell lines is a functional copy of the MLH1 gene, a gene which encodes for a nuclear MMR protein, the cell-selective behavior of our metalloinsertors must be related to this MMR deficiency. As the mitochondria are the location of oxidative phosphorylation, where reactive oxygen species are unavoidably formed as byproducts, mitochondrial DNA has higher levels of oxidative damage than nuclear DNA.[52] While these DNA defects could very well be targets of our metalloinsertors, mtDNA repair pathways do exist,[53] and in most cases are distinct from their nuclear counterparts.[54] Specifically, the nuclear MMR proteins MSH2, MSH3, MSH6, and MLH1 have been shown to be absent from the mitochondria.[55] The targeting of defects in mitochondrial DNA therefore cannot be responsible for the unique cell-selective behavior of our metalloinsertors. Instead, mitochondrial uptake appears to be associated with nonspecific toxicity.

CONCLUSION

In this work, all compounds tested are present in the nucleus at sufficient concentrations for mismatch detection. However, the more liphophilic compounds, which display enhanced uptake into the cells, tend to localize more in the mitochondria, thus giving rise also to nonspecific biological activity. While the more polar compounds ($[Rh(NH_3)_4(phzi)]^{3+}$, $[Rh(chrysi)(phen)(DPE)]^{3+}$, and $[Rh(DPAE)_2(chrysi)]^{3+}$) do not have the largest amount of cellular rhodium, there is consequently a smaller amount of rhodium in the mitochondria. This, coupled with sufficient nuclear rhodium for mismatch binding, gives rise to high MMR-deficient cell-selective biological activities for these three compounds. It seems that by increasing lipophilicity in an effort to increase uptake *via* passive diffusion, the subcellular localization is altered, leading to a larger amount of cellular rhodium residing in the mitochondria and less selectivity for the MMR-deficient cell line. This trade-off in uptake for selectivity is in contrast to current strategies to improve the efficacy of cisplatin by increasing uptake of the drug.[56,57] More generally, these results highlight that the relative accumulation of complex in different organelles needs to be considered, not simply cellular accumulation.

Most importantly, these data support the notion that the cell-specific activity we observe is caused by nuclear DNA mismatch targeting by our metalloinsertors. This exciting new result gives us key information in designing the next generation of rhodium metalloinsertors as cell-specific chemotherapeutics.

ASSOCIATED CONTENT

Supporting Information

Figures S1−S12, showing representative binding affinity determination, as well as inhibition of DNA synthesis by all 10 compounds at 6, 12, and 24 h of incubation. This material is available free of charge via the Internet at http://pubs.acs.org.

AUTHOR INFORMATION

Corresponding Author

jkbarton@caltech.edu

Notes

The authors declare no competing financial interest.

ACKNOWLEDGMENTS

Financial support for this work from the NIH (GM03339) is gratefully acknowledged. We also thank the National Science Foundation for a Graduate Research Fellowship to A.C.K. and the American Cancer Society for a Postdoctoral Fellowship to C.J.S. (118832-PF-10-017-01-CDD). This project benefitted from the use of instrumentation made available by the Caltech Environmental Analysis Center.

REFERENCES

(1) Kunkel, T. A.; Erie, D. A. *Annu. Rev. Biochem.* **2005**, *74*, 681−710.
(2) Loeb, L. A. *Cancer Res.* **2001**, *61*, 3230−3239.
(3) Bhattacharya, N. P.; Skandalis, A.; Ganesh, A.; Groden, J.; Meuth, M. *Proc. Natl. Acad. Sci. U.S.A.* **1994**, *91*, 6319−6323.
(4) Iyer, R. R.; Pluciennik, A.; Burdett, V.; Modrich, P. L. *Chem. Rev.* **2006**, *106*, 302−323.
(5) Arzimanoglou, I. I.; Gilbers, F.; Barber, H. R. K. *Cancer* **1998**, *82*, 1808−1820.
(6) Lawes, D. A.; SenGupta, S.; Boulos, P. B. *Eur. J. Surg. Oncol.* **2003**, *29*, 201−212.
(7) Carethers, J. M.; Hawn, M. T.; Chauhan, D. P.; Luce, M. C.; Marra, G.; Koi, M.; Boland, C. R. *J. Clin. Invest.* **1996**, *98*, 199−206.
(8) Fink, D.; Aebi, S.; Howell, S. B. *Clin. Cancer Res.* **1998**, *4*, 1−6.
(9) Aebi, S.; Fink, D.; Gordon, R.; Kim., H. K.; Zheng, H.; Fink, J. L.; Howell, S. B. *Clin. Cancer Res.* **1997**, *3*, 1763−1767.
(10) Jackson, B. A.; Barton, J. K. *J. Am. Chem. Soc.* **1997**, *119*, 12986−12987.
(11) Jackson, B. A.; Barton, J. K. *Biochemistry* **2000**, *39*, 6176−6182.
(12) Jackson., B. A.; Alekseyev, V. Y.; Barton, J. K. *Biochemistry* **1999**, *38*, 4655−4662.
(13) Junicke, H.; Hart, J. R.; Kisko, J.; Glevob, O.; Kirsch, I. R.; Barton, J. K. *Proc. Natl. Acad. Sci.U.S.A.* **2003**, *100*, 3737−3741.
(14) Pierre, V. C.; Kaiser, J. T.; Barton, J. K. *Proc. Natl. Acad. Sci. U.S.A.* **2007**, *104*, 429−434.
(15) Cordier, C.; Pierre, V. C.; Barton, J. K. *J. Am. Chem. Soc.* **2007**, *129*, 12287−12295.
(16) Zeglis, B. M.; Pierre, V. C.; Kaiser, J. T.; Barton, J. K. *Biochemistry* **2009**, *48*, 4247−4253.
(17) Song, H.; Kaiser, J. T.; Barton, J. K. *Nature Chem.* **2012**, *4*, 615−620.
(18) Lerman, L. S. *J. Mol. Biol.* **1961**, *3*, 18−30.
(19) Koi, M.; Umar, A.; Chauhan, D. P.; Cherian., S. P.; Carethers, J. M.; Kunkel, T. A.; Boland, C. R. *Cancer Res.* **1994**, *54*, 4308−4312.
(20) Hart, J. R.; Glebov, O.; Ernst, R. J.; Kirsch., I. R.; Barton, J. K. *Proc. Natl. Acad. Sci. U.S.A.* **2006**, *103*, 15359−15363.
(21) Gratzner, H. G. *Science* **1982**, *218*, 474−475.
(22) Ernst, R. J.; Song, H.; Barton, J. K. *J. Am. Chem. Soc.* **2009**, *131*, 2359−2366.
(23) Ernst, R. J.; Komor, A. C.; Barton, J. K. *Biochemistry* **2011**, *50*, 10919−10928.
(24) Golstein, P.; Kroemer, G. *Trends Biochem.* **2007**, *32*, 37−43.
(25) McCall, K. *Curr. Opin. Cell Biol.* **2010**, *22*, 882−888.

(26) Napolitano, S. M.; Aprille, J. R. *Adv. Drug Delivery Rev.* **2001**, *49*, 63−70.
(27) Klein, A. V.; Hambley, T. W. *Chem. Rev.* **2009**, *109*, 4911−4920.
(28) Ghezzi, A.; Aceto, M.; Cassino, C.; Gabano, E.; Osella, D. *J. Inorg. Biochem.* **2004**, *98*, 73−78.
(29) Puckett, C. J; Barton, J. K. *J. Am. Chem. Soc.* **2009**, *131*, 8738−8739.
(30) Pereira, M. P.; Kelley, S. O. *J. Am. Chem. Soc.* **2011**, *133*, 3260−3263.
(31) Meyer-Losic, F.; Quinonero, J.; Dubois, V.; Alluis, B.; Dechambre, M.; Michel, M.; Cailler, F.; Fernandez, A.-M.; Trouet, A.; Kearsey, J. *J. Med. Chem.* **2006**, *49*, 6908−6916.
(32) Keizer, H. G.; Schuurhuis, G. J.; Broxterman, H. J.; Lankelma, J.; Schoonen, W. G. E. J.; Rijn, J. v.; Pinedo, H. M.; Joenje, H. *Cancer Res.* **1989**, *49*, 2988−2993.
(33) Liu, J. L.; Galettis, P.; Farr, A.; Maharaj, L.; Samarasinha, H.; McGechan, A. C.; Baguley, B. C.; Bowen, R. J.; Berners-Price, S. J.; McKeage, M. J. *J. Inorg. Biochem.* **2008**, *102*, 303−310.
(34) Groessl, M.; Zava, O.; Dyson, P. J. *Metallomics* **2011**, *3*, 591−599.
(35) Zeglis, B. M.; Barton, J. K. *Nat. Protocols* **2007**, *2*, 357−371.
(36) Weidmann, A. G.; Komor, A. C.; Barton, J. K. *Philos. Trans. R. Soc. London, Ser. A.* **2012**. In press.
(37) Muerner, H.; Jackson, B. A.; Barton, J. K. *Inorg. Chem.* **1998**, *37*, 3007−3012.
(38) Basu, A.; Bhaduri, S.; Sapre, N. Y.; Jones, P. G. *J. Chem. Soc., Chem. Commun.* **1987**, *22*, 1724−1725.
(39) Reitmar, A. H.; Risley, R.; Bristow, R. G.; Wilson, T.; Ganesh, A.; Jang, A.; Peacock, J.; Benchimol, S.; Hill, R. P. *Cancer Res.* **1997**, *57*, 3765−3771.
(40) Mosmann, T. *J. Immunol. Methods* **1983**, *65*, 55−63.
(41) Ahmad, K. A.; Iskandar, K. B.; Hirpara, J. L.; Clement, M.-V.; Pervaiz, S. *Cancer Res.* **2004**, *64*, 7867−7878.
(42) Smith, P. K.; Krohn, R. I.; Hermanson, G. T.; Mallia, A. K.; Gartner, F. H.; Provenzano, M. D.; Fujimoto, E. K.; Goeke, N. M.; Olson, B. J.; Klenk, D. C. *Anal. Biochem.* **1985**, *150*, 76−85.
(43) ELISA data on five of these compounds have been reported previously in refs 22 and 36. However, the ELISA data reported here were obtained in parallel under the same conditions for all 10 metalloinsertors to verify trends.
(44) Puckett, C. A.; Barton, J. K. *J. Am. Chem. Soc.* **2007**, *129*, 46−47.
(45) Puckett, C. A.; Barton, J. K. *Biochemistry* **2008**, *47*, 11711−11716.
(46) Fujioka, A.; Terai, K.; Itoh, R. E.; Aoki, N.; Nakamura, T.; Kuroda, S.; Nishida, E.; Matsuda, M. *J. Biol. Chem.* **2006**, *281*, 8917−8926.
(47) Zhang, Y.; Lo, K. K-W. *Inorg. Chem.* **2009**, *48*, 6011−6025.
(48) Candeil, L.; Gourdier, I.; Peyron, D.; Vezzio, N.; Copois, V.; Bibeau, F.; Orsetti, B.; Scheffer, G. L.; Ychou, M.; Khan, Q. A.; Pommier, Y.; Pau, B.; Martineau, P.; Del Rio, M. *Int. J. Cancer* **2004**, *109*, 848−854.
(49) Eckford, P. D. W.; Sharom, F. J. *Chem. Rev.* **2009**, *109*, 2989−3011.
(50) Fink, D.; Nebel, S.; Aebi, S.; Zheng, H.; Kim, H. K.; Christen, R. D.; Howell, S. B. *Cancer* **1997**, *76*, 890−893.
(51) Horton, K. L.; Pereira, M. P.; Stewart, K. M.; Fonseca, S. B.; Kelley, S. O. *ChemBioChem* **2012**, *13*, 476−485.
(52) Yakes, F. M; Van Houten, B. *Proc. Natl. Acad. Sci. U.S.A.* **1997**, *94*, 514−519.
(53) Tomkinson, A. E.; Bonk, R. T.; Linn, S . *J. Biol. Chem.* **1988**, *263*, 12532−12537.
(54) Liu, P.; Demple, B. *Environ. Mol. Mutagen.* **2010**, *51*, 417−426.
(55) de Souza-Pinto, N. C.; Mason, P. A.; Hashiguchi, K.; Weissman, L.; Tian, J.; Guay, D.; Lebel, M.; Stevnsner, T. V.; Rasmussen, L. J.; Bohr, V. A. *DNA Repair* **2009**, *8*, 704−719.
(56) Fuertes, M. A.; Alonso, C.; Perez, J. M. *Chem. Rev.* **2003**, *103*, 645−662.
(57) Gately, D. P.; Howell, S. B. *Br. J. Cancer* **1993**, *67*, 1171−1176.